FACILE SYNTHESIS OFα-MoO_3/MnO_2 COMPOSITE ELECTRODES FOR HIGH PERFORMANCE SUPERCAPACITOR

Q. LI[a*], R. YAN[a], Y. F. ZHANG[b], L. M. DONG[a]
[a]*College of Materials Science and Engineering, Harbin University of Science & Technology Harbin, China*
[b]*AECC Harbin Dongan Engine Co.,LTD. , Harbin, China*

Supercapacitors (SCs), also named as electrochemical capacitors (ECs), have received much attention as one of the most significant energy storage devices with the rate of fast charge/discharge speed and non-pollution. In this work, the α-MoO_3 was synthesized by a simple electrospinning technique, and α-MoO_3/MnO_2 composite materials were synthesized by using a facile water bath method, where the MnO_2 microspheres grew uniformly around α-MoO_3 microchips. Morphology and structure of the samples are evaluated by scanning electron microscopy (SEM) and X-ray diffraction (XRD), respectively. Furthermore, the electrochemical properties of the samples were elucidated by cyclic voltammograms (CV) and electrochemical impedance spectroscopy (EIS) in 1 M NaOH electrolyte. The electrochemical results demonstrated that α-MoO_3 and α-MoO_3/MnO_2 composite materials exhibited specific capacitance of 76F/g and 109 F/g respectively at common scan rate of 10mv/s. The enhanced electrochemical behaviors could be ascribed to rational design of MnO_2 microspheres adhering on α-MoO_3 microchips, which supplies more pathways for accelerating fast electron and ion transfer by the synergistic effect of two electroactive materials. Indeed, these remarkable findings will enable low-cost α-MoO_3/MnO_2 attractive for high-performance supercapacitors.

(Received July 25, 2017; Accepted January 1, 2018)

Keywords: Supercapacitor, Specific capacitance, Composite, cyclic voltammetry

1. Introduction

Environmental deterioration is becoming more and more serious, and it is urgent to develop green energy storage equipment. Compared with common capacitors and batteries, supercapacitors (SCs)[1] attracted wide attention in the field of new energy with high power density, rate of fast charge and discharge speed, high cycle life and green environmental protection, etc[2-3]. However, low energy density limited its further application. As we know, the key to improve the supercapacitor energy density is to improve the specific capacitance of electrode material or improve the working voltage of the capacitor according to the energy density formula [4]. Electrochemical capacitor electrode materials are mainly divided into three kinds: carbon materials, metal oxides and conductive polymer materials [5]. Due to its high Faraday capacitance, transition metal oxides are considered as the most promising supercapacitor electrode materials for the next generation. Several traditional electrode materials such as RuO_2, NiO, Co_3O_4, MnO_2, MoO_3 and VO_x, etc are widely reported [5-7].

Among these electrode materials, MoO_3 has been widely used as electrode material in electrochemical energy storage devices, chemical/biological sensors, solar photovoltaic devices, optoelectronics, and electrodes [8]. MoO_3 is a kind of new material with unique one-dimensional layered structure. There are three mainly crystalline polymorphs of MoO_3: orthorhombic α-MoO_3 which is thermodynamically stable phase, monoclinic β-MoO_3 and hexagonal h-MoO_3 which are low temperature metastable phases. α-MoO_3 structures are precisely suitable for insertion/removal

* Corresponding author:qinalily@163.com

of small ions such as H^+ and Na^+ due to its layered structure along its [010] direction[9].

Although α-MoO_3 is an electrode material with high theoretical capacitance and good cycle stability, the ionic and electronic conductivity is relatively poor. On the other hand, MnO_2 has high ionic and electronic conductivity [10-12]. So, in this work, we report the fabrication of composites with MnO_2 deposited on MoO_3 and demonstrate the out-standing capacitive performance of the as-prepared composites.

2. Experimental

2.1 Preparation of α-MoO_3 and MoO_3/MnO_2 materials

Firstly, α-MoO_3 was prepared by electrospinning. 1g Ammonium heptamolybdate tetrahydrate $(NH_4)_6Mo_7O_{24}\cdot 4H_2O$ (EP, Tianjin Guangfu Fine Chemical Research Institute) was dissolved in the mixture of 10 ml deionized water and 15 ml ethanol. After magnetic stirring for 2 h, 3 ml ammonia (AR) and 1.5 g PVP (aladdin, Mw = 1300000) was slowly added into the above solution. Then the solution was sucked into a plastic syringe with a stainless steel needle with an inner diameter of 0.5 mm. The electrospun membranes were produced at an applied voltage of 30 kV and a distance of 13 cm between the needle tip and aluminum foil collector. The as-prepared membranes were then annealed to 600 ^oC with the heating rate of 3 ^oC/min and hold there for 3 h in air to obtain the MoO_3 fibers.

Second, 0.5 g α-MoO_3 fibers were dispersed in 60 mL deionized water with ultrasonic treatment for 30 min. Secondly, 0.22 g $KMnO_4$ and 0.28 g $MnSO_4$ (EP, Tianjin Guangfu Fine Chemical Research Institute) and 0.6 mL HNO_3 (65%) were dissolved into the solution. The products were centrifugal separated, washed and dried. Finally the products were annealed at 300 ^oC for 2 h with the heating rate of 3 ^oC/ min in air.

2.2 Materials characterization

The morphology of samples was observed by a scanning electron microscope (SEM; Sirion200, Philip). The crystalline structure of samples was determined by power X-ray diffraction (Shimadzu, XRD-6000, Cu Ka target). Electrochemical tests including cyclic voltammetry (CV) curve and electrochemical impedance spectroscopy (EIS) tests were carried out using three electrode test system with 1M NaOH as electrolyte by RST5000 electrochemical workstation (Ruisite Instrument, Suzhou). The samples were used as the working electrodes, and a standard calomel electrode (SCE) and Pt sheet were used as the reference and counter electrodes, respectively.

The working electrode was prepared by mixing with conductive carbon black (super P) and Polytetrafluoroethylene (PTFE) as the binder in the weight ratio of 8:1:1. Then, the resulting mixture was coated onto the Ni foam substrate of 10 mm × 10 mm square, which was used as the current collector. The foam was dried at 60 °C for 12 h in air to evaporate the solvent. The voltage window of cyclic voltammograms (CVs) was 0−0.8 V with different scan rates ranging from 10 to 100 mv/s. The electrochemical impedance spectroscopy (EIS) measurements were conducted by applying an AC voltage in the frequency range from 10 mHz to 100 kHz with 5 mV amplitude. The specific capacitance (Cs) was calculated using the galvanostatic charge/discharge data according to the following equation[13]:

$$c = \frac{\int \mathrm{I} dV}{2m\nu\Delta U} \tag{1}$$

Where $\int Idv$ is CV Integral area of curve, m is active material quality, V is scanning speed, ΔU is potential window.

3. Results and discussion

3.1 Phase Identification and Crystal Structure

Phase analysis of the powders was carried out by XRD. Figure 1 shows the XRD pattern of the MoO_3 and MoO_3/MnO_2. The test result is compared with JCPDS card. All the diffraction peaks correspond to the MnO_2 crystal, diffraction peaks at 28.7°, 37.3°, 56.7°, and 72.4° are successively ascribed to the (110), (101), (211), and (112) diffraction (JCPDS file No.24–0735). After the follow water bath step, the MoO_3/MnO_2 diffraction peaks at 12.8°, 23.3°, 25.7°, 27.3°, 33.7°, 38.9° are successively ascribed to the (020), (110), (040), (021), (111) and (060) diffraction (JCPDS file No.05–0508). No other peaks for impurities were observed.

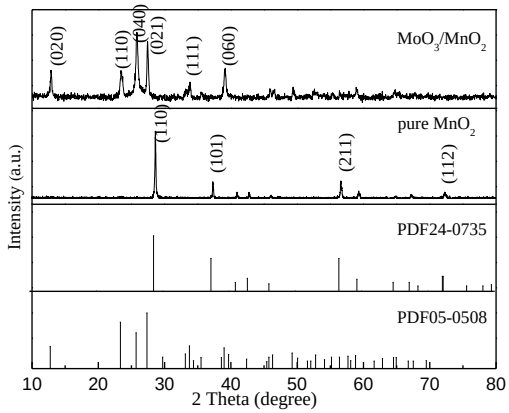

Fig. 1. XRD patterns of pure MnO_2 and α-MoO_3/MnO_2

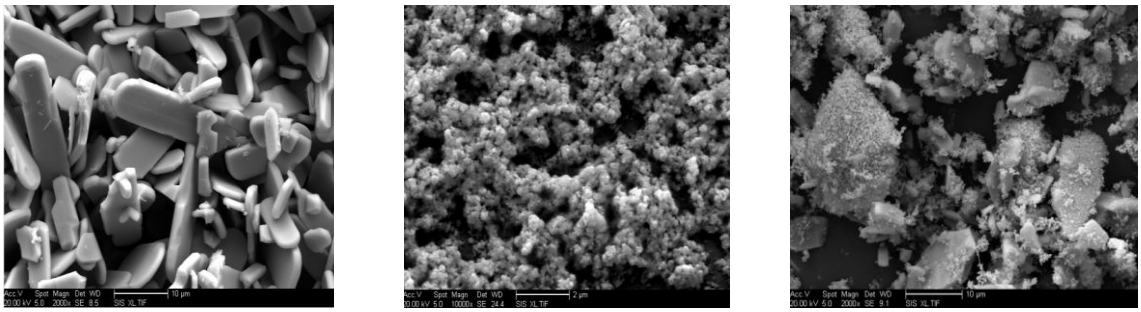

a) b) c)

Fig. 2: (a) SEM image of pure α-MoO_3 microchips. (b) SEM image of pure MnO_2 microspheres. (c) α-MoO_3/MnO_2 compound material

Fig. 2 shows the SEM images of α-MoO_3 and α-MoO_3/MnO_2 morphologies. Fig. 2a and Fig. 2b show the SEM images of α-MoO_3 microchips and MnO_2 microspheres, respectively. High magnification images indicate that the α-MoO_3 microchips possess average diameter of several micrometers and MnO_2 microspheres have a relative uniform diameter of about 500-700 nm. From Fig. 2c, we can observe that α-MoO_3 microchips are coated by MnO_2 microspheres. The high magnification images of individual samples showed that the α-MoO_3 microchips are self-assembled by some small nanospheres. After the hydrothermal reaction with $KMnO_4$ and $MnSO_4$, the surface of α-MoO_3 microchips was evenly decorated by some MnO_2 microspheres.

3.2 Electrochemical measurement

Fig. 3 shows the cyclic voltammetry (CV) curves at different scan rates. As we can see from the diagram, the cyclic voltammetry curves have no regular rectangular feature and there are obvious redox peaks.

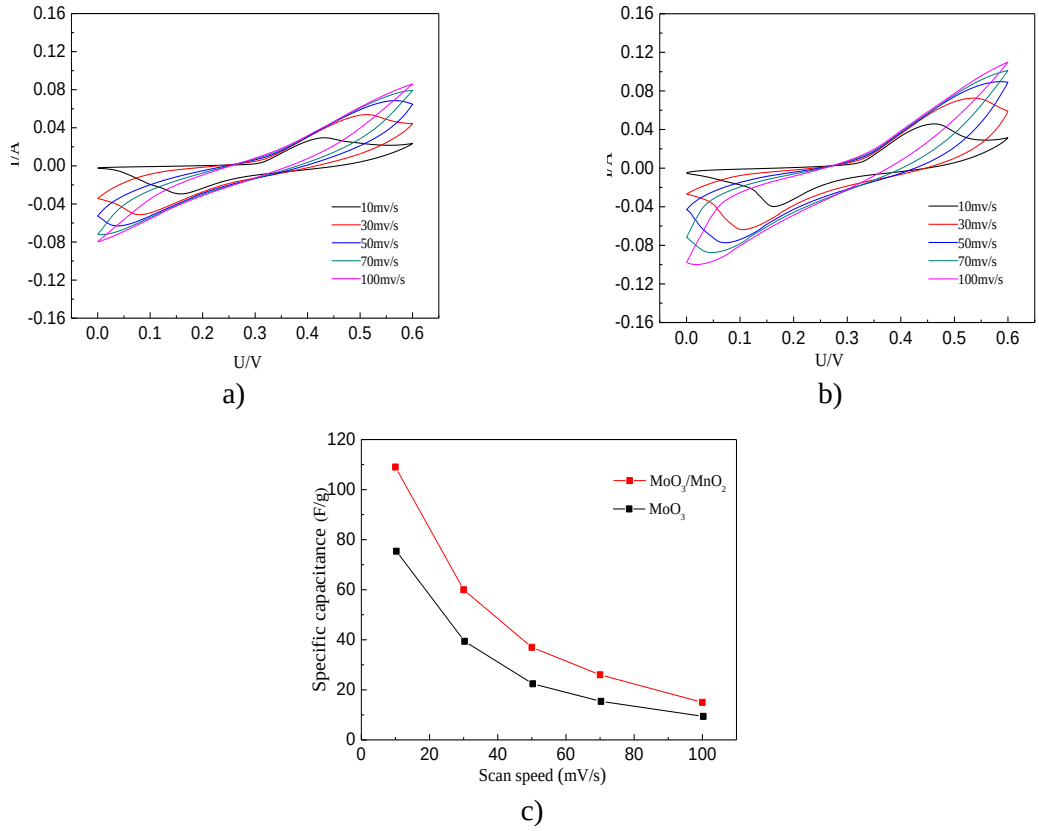

Fig. 3. (a) CV curves of the α-MoO_3 at the different scan rates. (b) CV curves of the α-MoO_3/MnO_2 at the different scan rates. (C)Capacitance of the α-MoO_3 and α-MoO_3/MnO_2 at different scan rates

There are obvious redox peaks at 0.15 V and 0.45 V, indicating that pseudo potential is generated near this potential. The redox peak becomes less pronounced and the specific capacitance decreases continuously. The specific capacitance of two electrodes at various scan rate were calculated, α-MoO_3 possess specific capacitance of 76 F/g and α-MoO_3/MnO_2 composites show their specific capacitance of 109 F/g at scan rate of 10 mV/s. After scanning with the rates from 10 to 100 mV/s, the specific capacitance of the composite only maintains 20% of initial specific capacitance, suggesting that the composite material could not undergo bigger scan rates and keep steady electrochemical performance.

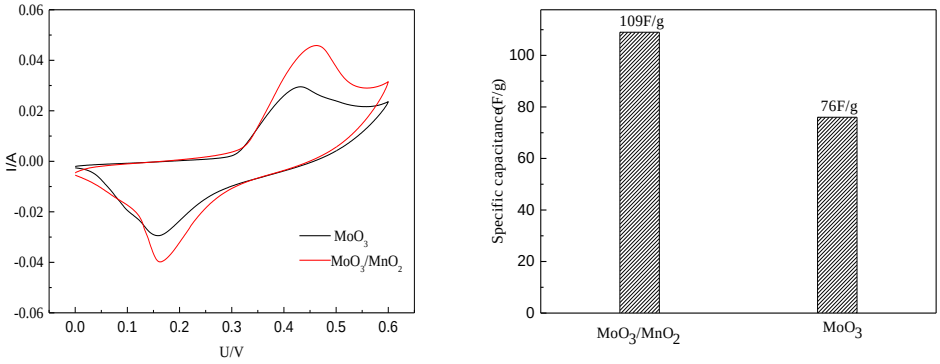

a) *b)*

Fig. 4. (a) CV curves of the MoO_3 and MoO_3/MnO_2 at scan rate of 10mV/s; (b) The calculated specific capacitance of MoO_3 and MoO_3/MnO_2 at scan rate of 10mV/s.

Therefore α-MoO_3/MnO_2 composites will have high capacity [14-15], good stability and high rate capability, which is attributed to the synergistic effect of the two mechanisms. The material of metal oxide based electrodes rely on Faraday reaction to provide capacitance properties [16-19], including chemical adsorption occurs only between the active material of NaOH electrolyte and electrode surface insertion/removal phenomenon, as shown in the following equations [20]:

$$(MoO_3)_{surface} + xC^+ + xe^- \longleftrightarrow (C_xMoO_3)_{surface}, \quad C = H, Li^+, K^+ \text{ and } Na^+ \tag{2}$$

$$(MnO_2)_{surface} + C^+ + e^- \longleftrightarrow (MnOOC)_{surface}, \quad C = H, Li^+, K^+ \text{ and } Na^+ \tag{3}$$

also including the chemical adsorption can occur between electrolyte and internal active material, see equation (4) (5):

$$MoO_3 + xC^+ + xe^- \longleftrightarrow C_xMoO_3 \quad C = H, Li^+, K^+ \text{ and } Na^+ \tag{4}$$

$$MnO_2 + C^+ + e^- \longleftrightarrow MnOOC \quad C = H, Li^+, K^+ \text{ and } Na^+ \tag{5}$$

From the above equation (2) and (3), it can be seen that this reaction occurs only on the electrode surface, so the increase of the specific capacitance of the electrode material can be achieved by improving the specific surface area of the electrode material. α-MoO_3/MnO_2 composite can not only have more contact area of electrode and electrolyte, but also have better electrochemical performance.

Figure 4a shows the cyclic voltammetry curves of α-MoO_3 and α-MoO_3/MnO_2 over a voltage ranging from 0 to 0.6 V at scan rate of 10 mV/s. It is easy to distinguish that the enclosed area of α-MoO_3 was smaller than α-MoO_3/MnO_2 composites, which shows α-MoO_3/MnO_2 composites delivered more outstanding capacitance than individual α-MoO_3. The calculated specific capacitance of α-MoO_3 and α-MoO_3/MnO_2 was 76 F/g, 109 F/g by equation as shown in figure 4b. The compound material displayed higher specific capacitance and electrochemical performance than pristine α-MoO_3, indicated that the composite of two metal oxides can improve the electrochemical properties of the electrode material, owing to MnO_2 has high ionic and electronic conductivity and remarkable chemical stability.

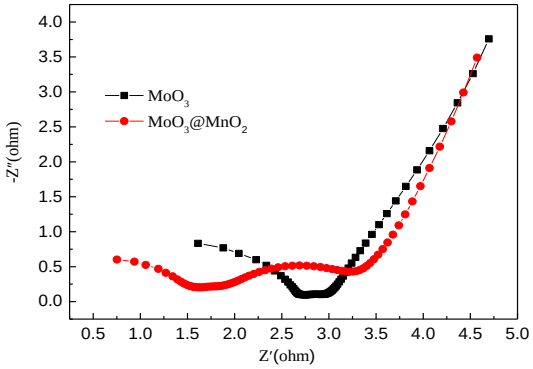

Fig. 5. AC impedance spectra of MoO_3 and MoO_3/MnO_2

Fig. 5 shows the electrochemical impedance spectra (EIS) of both the α-MoO_3 and α-MoO_3/MnO_2 in the frequency range of 100000Hz-0.01Hz. The electrochemical impedance spectra (EIS) consist of a semicircle and an oblique line. The diameter of high frequency semicircle is mainly related to the transfer resistance of the charge. The diameter of the semicircle is greater shows that the transfer resistance is larger. The tilt angle of the oblique line is mainly related to the diffusion resistance of the ion. The larger the angle is, the smaller the resistance of the active material is. As a consequence, the diameter of the semicircle for α-MoO_3/MnO_2 is smaller than that of the α-MoO_3 and the tilt angle of the oblique line for α-MoO_3/MnO_2 is bigger than that of the α-MoO_3. It indicates that the α-MoO_3/MnO_2 materials are beneficial to enhance the reaction kinetics and better electrochemistry performance of the supercapacitors.

At the very low frequency region, the straight line with a large slope demonstrates a good capacitive behavior without diffusion limitation. At the high frequency region, the bigger diameter of the semicircle for MoO_3/MnO_2 confirmed the reasons for the increase of the capacitance. In addition, the MnO_2 microspheres coated on MoO_3 microchips can shorten the diffusion path of ions, the active material and electrolyte ions contact effectively. The composite material provides better conductivity, multiple valence bands and more environments for reversible redox reaction. The enhanced capacitance of MoO_3/MnO_2 can also be explained by the interfacial charging mechanism which obviously increase the whole surface area and provide more electrochemical active sites. Much interfacial space between MnO_2 and a-MoO_3 can probably accommodate extra ions. More ions and electrons can be inserted in the boundary region of a-MoO_3/MnO_2 and a great potential for interfacial storage of ions and electrons can improve the electrochemical capacity.

4. Conclusions

In conclusion, α-MoO_3/MnO_2 was successfully prepared by electrospinning and water bath. The results indicate that α-MoO_3/MnO_2 exhibits good cycling performance and excellent electrochemical behavior. This is attributed to the synergetic effect of α-MoO_3 and MnO_2 as well as the assembled heterojunction. The assembled heterojunction supply more pathways and lager surface area for transfer of the charge and diffusion of the ion. Moreover, composite oxide of two or more types of metal can further improve the electrochemical capacitor energy density and cycle performance. It also provides a new direction for the study of electrochemical capacitors with excellent performance.

Acknowledgment

This work was financially supported by special fund project for technology innovation talents of Harbin (2016RQQXJ137).

References

[1] H. Wu, Z. Lou, H. Yang, et al. Nanoscale, **7**, 1921 (2015).
[2] W. Ma, H. Nan, Z. Gu, et al. Journal of Materials Chemistry A, **3**, 5442 (2015).
[3] M. Huang, Y. Zhang, F. Li, et al. Journal of Power Sources, **252**:98 (2014).
[4] G. S. Gund, D. P. Dubal, N. R. Chodankar, et al. Scientific Reports, **5**, 12454 (2014).
[5] Y. Shi, B. Guo, S. A. Corr, et al. Nano Letters, **9**, 4215 (2009).
[6] H. T. Cui, M. M. Wang, W. Z. Ren, et al. Functional Materials Letters, **7**, 1450002 (2014).
[7] F. Qu, J. Liu, Y. Wang, et al. Sensors & Actuators B Chemical, **199**, 346 (2014).
[8] Q. D. Yang, H. T. Xue, Y. Xia, et al. Electrochimica Acta, **185**, 83 (2015).
[9] Y. Liu, B. Zhang, Y. Yang, et al. Journal of Materials Chemistry A, **1**, 13582 (2013).
[10] Y. wen, T. Qin, Z. Wang, et al. Journal of Alloys and Compounds, **699**, 126 (2017).
[11] Q. Chen, B. Heng, H. Wang, et al. Journal of Alloys & Compounds, **641**, 80 (2015).
[12] J. G. Wang, Y. Yang, Z. H. Huang, et al. Electrochimica Acta, **75**, 213 (2012).
[13] C. Yang, Y. Shi, N. Liu, et al. Rsc Advances, **5**, 45129 (2015).
[14] Y. Duan, J. Chen, Y. Zhang, et al. Journal of Superconductivity and Novel Magnetism, **27**, 2139 (2014).
[15] M. Zhi, A. Manivannan, F. Meng, et al. Journal of Power Sources, **208**, 345 (2012).
[16] G. Chen, S. Wu, L. Hui, et al. Scientific Reports, **6**, 19028 (2016).
[17] H. Xia, D. Zhu, Z. Luo, et al. Scientific Reports, **3**, 2978 (2013).
[18] L. Fei. Study on the Hydrothermal Synthesis and electrochemical Properties of MnO_2(D), Taiyuan University of Technology, (2015)
[19] Y. He, W. Chen, X. Li, et al. Acs Nano, **7**, 174 (2013).
[20] Q. Wang, D. A. Zhang, Q. Wang, et al. Electrochimica Acta, **146**, 411 (2014).